

# Image-guided, surgical robot-assisted percutaneous puncture of the foramen ovale and foramina stylomastoideum: a cadaveric study

Fan-Hao Meng<sup>1</sup>, Yu Song<sup>2</sup>, Bo Qiao<sup>1</sup>, Neng-Hao Jin<sup>1</sup>, Yan-Ming Zhu<sup>3</sup>, Bo-Fu Liang<sup>4</sup>, Deng-Fa Gao<sup>3</sup>, Hai-Zhong Zhang<sup>1</sup>

<sup>1</sup>Department of Oral Maxillofacial Surgery, Chinese PLA General Hospital, Beijing 100853, China;

<sup>2</sup>Department of Oral Implantology, Beijing Ruicheng Stomatology Hospital, Beijing 100032, China;

<sup>3</sup>Department of Radiology, Chinese PLA General Hospital, Beijing 100853, China;

<sup>4</sup>Beijing Baihui Weikang Technology Co., Ltd., Beijing 100080, China.

Surgical robots have been widely used in surgery. Currently, the da Vinci Surgical System (Intuitive Surgery, Inc., Sunnyvale, CA, USA) is the most common robotic system used in the clinical setting. This system has proven useful for lesions in occult positions, such as tumors at the base of the tongue, ranulas, and submandibular lithiases. It is less traumatic compared to traditional open surgical procedures; however, its suitability for punctures remains debatable. Remebot (Beijing Baihui Weikang Technology Co., Ltd.; Beijing, China) is a surgical robot that is currently being used for neurosurgical procedures. Based on the intra-operational navigation, it can aid the surgeon with both the direction and depth of puncture, simultaneously. Although it can reportedly achieve an accuracy of  $1.330 \pm 0.566$  mm<sup>[1]</sup> in biopsy operations, the same has not been reported in the field of oral and maxillofacial surgery. Therefore, in order to verify the feasibility of using a robot in oral and maxillofacial surgery, we chose to puncture the foramen ovale (FO) and foramina stylomastoideum (FS) in the present study.

The FO is located in the large wing (near the body) of the sphenoid bone, in front of the spinous foramen, and posterolateral to the foramen rotundum. The mandibular nerve exits the FO and enters the infratemporal fossa. In the clinical setting, the treatment of trigeminal neuralgia often involves a percutaneous puncture of the FO. However, it is difficult to successfully puncture the FO in a single attempt because of its location deep within the human body; moreover, the puncture path faces obstruction from the upper and lower jaws, thereby reducing the actual effective puncture angle.

The FS is located on the lateral side of the skull base, between the styloid process and the mastoid process of the

temporal bone and behind the root of the styloid process. It acts as the external opening of the facial nerve canal and extends vertically upward to join with the canal. Adenoid cystic carcinoma of the parotid gland can easily develop inside the FS along the facial nerve owing to its neurophilic and fast-growing nature. However, it is sensitive to radiotherapy; brachytherapy seeds implanted into the FS can control tumor progression.

Only a few studies have reported the use of a robotic system in the maxillofacial region. Thus, this study aimed to verify the accuracy and feasibility of the application of Remebot in the field of oral and maxillofacial surgery by puncturing the FO and FS.

The following materials were used in this study: Remebot, Kirschner wire, and 11 cadaveric heads fixed in 10% buffered formalin. All specimens were from voluntary donation and obtained by Department of Anatomy of Peking Union Medical College. The study protocol was approved by the Institutional Review Board of General Hospital of the People Liberation Army (No. S2018-281-02).

The surface of each cadaveric head was cleaned before the surgery. Three fiducial markers containing ceramic balls were pasted onto the frontal and bilateral temporal regions of a cadaveric head. Owing to difficulties in pasting the markers, bone nail markers were used for the remaining specimens. It is important to note that the three points should not be collinear and four points should not be coplanar while placing the markers. The specimen was placed in a supine position. Subsequently, pre-operative volumetric thin-layer computed tomography (CT) scanning of the cadaveric head was performed. Each head was placed in a holder to fix its spatial position. Digital Imaging

## Access this article online

Quick Response Code:



Website:

www.cmj.org

DOI:

10.1097/CM9.0000000000001783

**Correspondence to:** Hai-Zhong Zhang, Department of Oral Maxillofacial Surgery, Chinese PLA General Hospital, Beijing 100853, China  
E-Mail: zhang126301@126.com

Copyright © 2021 The Chinese Medical Association, produced by Wolters Kluwer, Inc. under the CC-BY-NC-ND license. This is an open access article distributed under the terms of the Creative Commons Attribution-Non Commercial-No Derivatives License 4.0 (CCBY-NC-ND), where it is permissible to download and share the work provided it is properly cited. The work cannot be changed in any way or used commercially without permission from the journal.

Chinese Medical Journal 2021;134(19)

Received: 24-04-2021 Edited by: Ning-Ning Wang

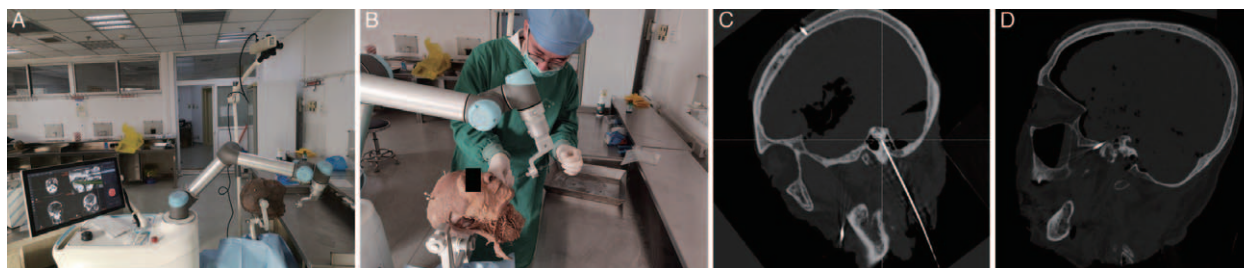


**Figure 1:** Illustration of image-guided, surgical robot-assisted percutaneous puncture of the FO and FS. (A) The layout of robotic arm, a computer, an optical pose tracker, mobile trolley, and specimen. (B) Under the guidance of the robotic arm, the doctor punctured the needle in the direction and depth indicated. (C) Post-operative CT showed the needle had been punctured into FS successfully. (D) Post-operative CT showed the needle had been punctured into FO successfully. CT: Computed tomography; FO: Foramen ovale; FS, Foramina stylomastoideum.

and Communications in Medicine data were imported to the Remebot-dedicated software and reconstructed. The FO and FS were identified on the base of the skull. The trajectories for bilateral percutaneous puncture of the FO and FS were planned on different views using 3D reconstructed objects. The Hartel anterior approach was used as a reference to design the pathway for the percutaneous puncture of the FO.

After the registration of the data, the robotic arm was made to pre-demonstrate the operating path to ensure no obstruction during the procedure [Figure 1A]. During the operative phase, the robotic arm moved to the pre-determined path with an accurate orientation toward the trajectory. The movement could be controlled by the surgeon using three available modes (point-to-point, axial, and free). An optimal-sized Kirschner wire was selected for use during the percutaneous puncture under the guidance of the robotic arm [Figure 1B]. The default puncture depth of the robotic arm was set at 15 cm; hence, the same measurement was used to mark the depth on the Kirschner wire. When the needle was punctured to the pre-determined depth, the split-type manipulator was detached, and the Kirschner wire was left in place. The same method was repeated for the contralateral puncture.

The split-type end of the robotic arm was designed to retain the Kirschner wire in place after the puncture. CT scans were taken after completing the percutaneous punctures on both sides and the images were imported into a professional software program to determine the puncture points in the reconstructed objects [Figure 1C, D]. The location errors were calculated by comparing the preoperative plan with the post-actual puncture point. The Euclidean distances between the centers of the FO and FS and the tip of the needle were measured in the IBM SPSS 20 software (IBM Corp., Armonk, NY, USA). Paired *t* test can be used for investigate the difference of the puncture results between two sides.

Twenty-two sides were successfully punctured in the FO. The average accuracy of the FO puncture of left side and right side were  $1.49 \pm 0.51$  mm and  $1.31 \pm 0.61$  mm, respectively ( $P = 0.445$ ). The errors of the puncture skin point of left side and right side were, respectively,  $1.35 \pm 0.83$  mm and  $1.86 \pm 0.80$  mm ( $P = 0.230$ ). After preoperative scanning, three of 11 specimens were found to have been destroyed in petrous part and tympanic part

of temporal bone. Thus, a total of 16 sides of stylomastoid foramen puncture were performed. The accuracy of the FS puncture target of left side and right side were, respectively,  $1.35 \pm 0.87$  mm and  $1.77 \pm 1.13$  mm ( $P = 0.105$ ). According to the above three results, there was no significant difference between two sides.

Clinically, we attempt to implant the brachytherapy seeds into the facial nerve canal for the limitation of tumor growth. The diameter of the FS decreases from the root of the styloid process to the cranial side on the thin-layer CT. It traverses up vertically into the facial canal and gradually narrows in width. Therefore, it is difficult to puncture the FS in a single attempt.

The FO transmits the mandibular division of the trigeminal nerve, the accessory meningeal artery, and the emissary veins between the cavernous sinuses and the pterygoid plexus. The average length and width of the FO are 6.4 and 3.2 mm, respectively.<sup>[2]</sup> The maximum longitudinal diameter of the FO is the most important factor that contributes to the difficulties during puncture. Currently, the Hartel anterior approach is the most commonly used method to access the FO. However, anatomic variations of the FO can potentially lead to unsuccessful cannulation. FO cannulation using the Hartel approach yields a 5.17% failure rate due to anatomic variations in FO morphology,<sup>[3]</sup> despite the use of neuro-navigation technology with CT imaging. Generally, percutaneous procedures are “blinded” by definition. Furthermore, CT-guided puncture of the FO is another commonly used method for the accurate percutaneous treatment of the FO.<sup>[4]</sup> With the help of the navigation system, surgeons could identify the position of the needle through intra-operative CT examination. In a study by Fransen,<sup>[5]</sup> the mean radiation dose per patient during percutaneous balloon compression of the trigeminal ganglion was reported to be  $1137.18$  mGy cm<sup>2</sup> (range, 639.50–1738.00 mGy cm<sup>2</sup>). Therefore, the radiation required to perform this procedure might pose a significant risk for both the surgeon and the patient.

Compared to the two aforementioned methods, the major advantage of the surgical robot-assisted system is that surgeons can design and navigate the pathway of puncture based on their own CT data. This reduces the risks of a blinded operation during percutaneous puncture. The presence of anatomical variations can be detected before surgery, and a personalized pathway can be designed to

improve the success rate of the percutaneous puncture. The depth and direction of the percutaneous puncture can be simultaneously indicated during robotic surgery. The Remebot can locate the end of the robotic arm, which is set at 15 cm away from the target point, with high precision. The surgeon only needs to place the puncture needle through the end of the robotic arm and puncture it along the pre-determined direction. CT guidance requires repeated CT examination intra-operatively to identify the position of the tip of the puncture needle, which increases the risk of radiation exposure. In the case of the Remebot, the patient only needs to undergo a pre-operative CT scan once, on the day of the surgery. By analyzing the experimental results, the Remebot can fulfill the requirements of the FO and FS percutaneous puncture. Furthermore, the robotic-assisted system can greatly lower the skill barrier to perform the percutaneous puncture. Thus, a surgeon with limited experience can accomplish a successful puncture with the assistance of the Remebot.

The conventional navigation system requires skin preparation of the whole head followed by its fixation on a holder. It is agonizing for most patients who undergo oral and maxillofacial surgery to have their heads shaved bald. Therefore, we modified the method of registration, wherein only the temporal hair needs to be shaved off, on both sides. The Remebot could identify the markers, which consisted of black and white blocks, through the optical tracking system. However, owing to the invasive nature of this method, we aim to develop a non-invasive method for the fixation and registration of the head in the future.

This study has some limitations. Simulating intra-operative bleeding in actual surgical scenes was not possible in the cadaveric specimens used in this study. During cannulation in the Hartel approach, three anatomical structures—the cheek, the pterygomaxillary fossa, and finally the FO—will need to be successively traversed. Thus, the possibility of the needle piercing the internal carotid artery, maxillary artery, middle meningeal artery, or pterygoid venous plexus exists. However, the Remebot could integrate multimodal images, including the magnetic resonance imaging and CT data, to fully design the optimal puncture trajectory in this study. In the future, comparative studies using larger sample sizes are warranted to verify the advantage of a CT-guided, surgical robot-assisted system.

This study verifies the feasibility and accuracy of using a robot in the field of oral and maxillofacial surgery. The puncture results of the FO and FS in the cadaveric specimens confirm that this method meets the requirements of clinical surgery.

### Funding

This study was supported by the grants from the National Key Research and Development Plan (No. 2017YFB1304300), the Conversion Fund of PLA General Hospital (2017tm-018), the Clinical Research Support Fund of PLA General Hospital (2017fc-tsys-2013), and the Research on Big Data Sharing Service Platform for Oral Cancer Imaging (2018mbd-13).

### Conflicts of interest

None.

### References

1. Wang T, Zhao QJ, Gu JW, Shi TJ, Yuan X, Wang J, *et al.* Neurosurgery medical robot Remebot for the treatment of 17 patients with hypertensive intracerebral hemorrhage. *Int J Med Robot* 2019; 15:e2024. doi: 10.1002/rcs.2024.
2. Luo C, Zhang Y, Luo GX, Wang M. Research progress in treatment of trigeminal neuralgia by percutaneous compression of semilunar ganglion with micro-balloon compression (in Chinese). *Chin J Clin Neurosurg* 2019;6:371–374. 377. doi: 10.13798/j.issn.1009-153X.2019.06.018.
3. Filippiadis DK, Markoutsas D, Mazioti A, Tsoukalos G, Papakonstantinou O, Stamatis P, *et al.* Computed tomography-guided radiofrequency thermocoagulation of the Gasserian ganglion using an alternative to Hartel anterior approach: a bicentral study. *Pain Physician* 2020;23:293–298.
4. Mandat T, Brozyna B, Krzymanski G, Podgorski JK. An image-guided, noninvasive method of cannulation of the foramen ovale for awake, percutaneous radiofrequency rhizotomy. *J Neurosurg* 2009;111:1223–1225. doi: 10.3171/2009.1.JNS0852.
5. Fransen P. Fluoroscopic exposure during percutaneous balloon compression of the Gasserian ganglion. *J Neurointerv Surg* 2013; 5:494–495. doi: 10.1136/neurintsurg-2012-010370.

How to cite this article: Meng FH, Song Y, Qiao B, Jin NH, Zhu YM, Liang BF, Gao DF, Zhang HZ. Image-guided, surgical robot-assisted percutaneous puncture of the foramen ovale and foramina stylo-mastoid: a cadaveric study. *Chin Med J* 2021;134:2362–2364. doi: 10.1097/CM9.0000000000001783